Colloid Polym Sci (2006) 284: 1431–1442
DOI 10.1007/s00396-006-1521-8

ORIGINAL CONTRIBUTION

Isabel Díez
Klaus Tauer
Burkhard Schulz

Unusual polymer dispersions—polypyrrole suspensions made of rings, frames, and platelets

Received: 13 April 2006
Accepted: 12 May 2006
Published online: 24 June 2006

I. Díez · B. Schulz
University of Potsdam Institute
of Physics Am Neuen Palais 10,
Haus 19,
D-14469 Potsdam, Germany

K. Tauer (✉)
Max Planck Institute of Colloids
and Interfaces Am Mühlenberg,
D-14476 Golm, Germany
e-mail: klaus.tauer@mpikg-golm.mpg.de

Abstract Experimental results show that the polymerization of pyrrole in the presence of β-naphthalenesulfonic acid and different fluorosurfactants like perfluorooctanesulfonic acid, perfluorooctyldiethanolamide, and ammonium perfluorooctanoate leads to polypyrrole with special morphologies, such as rings or disks and rectangular frames or plates. The formation of these unusually shaped particles of polymer dispersions is explained by the chemical and colloidal peculiarities of the oxidative pyrrole polymerization with ammonium peroxodisulfate in aqueous medium.

Keywords Polypyrrole · Chemical oxidative polymerization · Particle morphology

Introduction

Among the conducting polymers, polypyrrole (PPY) has attracted much attention because of its good environmental stability and high conductivity [1]. Together with its facile synthesis, the polymer is considered to be a promising material for uses in biosensors [2], electronic devices, batteries, and displays [3]. The oxidative (either chemically or electrically initiated) polymerization of pyrrole leads, in the absence of any additives, to polymer with only poor processibility [4] and typical granular morphology.

Nowadays, besides cases where the polymer is electrochemically deposited on a substrate directly in the final application form, any processing method for conducting polymers uses dispersions [5]. The polymers in the form of dispersions are easy to shape on minimum-length scales represented by the average size of the dispersed particles.

To render the polymer conducting and to improve the processibility of the material, polymerizations were carried out in the presence of different sulfonic acids as additives. This so-called in situ doping resulted in PPY with different solubility [6] and morphology. For example, PPY synthesized in the presence of ammonium peroxodisulfate (APS) as oxidant and β-naphthalenesulfonic acid (NSA) as dopant possesses fibrillar morphology, whereas many other sulfonic acid dopants lead to polymers with ordinary granular morphology. It is also reported that in situ sulfonation with fluorosulfonic acid (FSO_3H) during the electrochemical synthesis causes the formation of a polymer with fibrillar morphology and increased electrical conductivity [7]. Moreover, the synthesis of PPY in low-molecular-weight micellar surfactant solutions [8–11], in block copolymer micelles [12–15], in admicelles [16], and in the presence of a pyrrole-modified poly(vinyl alcohol) as reactive stabilizer [17] is described. But in all of these cases, and without the application of additional means, the PPY is formed with a granular shape. Only one patent mentions the addition of fluorosurfactants to solutions or dispersions of PPY, but only after polymerization [18].

Moreover, the morphology or the shape of the PPY can be tuned relatively easy both macroscopically and micro- or nanoscopically in very different ways by the application of the corresponding templates, which neither participate directly in the polymerization reaction nor influence the chemical structure. The templates can, if necessary, be removed again in the majority of the cases after the polymerization. Examples of such external morphological templates are polymer films [19, 20], cotton fabrics [21], gas or liquid interfaces [22], glass substrates coated with poly(styrene sulfonate) [23] or modified with octadecyl

chains or hydroxyl groups [24], polymeric or inorganic colloidal particles [25], and the surfaces and interstitial volumes in latex crystals leading to inverse PPY opals [26, 27]. This is only a selection of interesting cases without claiming completeness.

There is another type of morphology control where the template is formed in situ by the recipe components at the beginning of the polymerization. This "in situ templating" was first observed for the polymerization of aniline, as described by Shen and Wan [6], and also recently for pyrrole [28]. It was shown that the fibrillar morphology of PPY resulted from casting of a pyrrole-NSA complex, which is formed prior to polymerization. At the end of the polymerization, the pyrrole-NSA complex can easily be removed by washing with ethanol, and hollow PPY shells remain.

Particularly, this contribution reports on the influence of various fluorosurfactants on the morphology of PPY as obtained by oxidative polymerization with APS in the presence of NSA. The particular morphologies are strongly dependent on the nature of the hydrophilic group of the perfluoroalkyl surfactant, as it is found for perfluorooctanesulfonic acid (PFOSA), ammonium perfluorooctanoate (APFO), and perfluorooctyldiethanolamide (PFODEA).

Experimental part

Materials

Pyrrole (Acros) was, if necessary, distilled (dark brownish batches of the monomer) or used as received and stored in a refrigerator until use. NSA (Acros, melting point 77–79 °C) and APS (Aldrich) were used as received. For all calculations, the molecular weight of NSA was assumed to be 226.25 g mol^{-1}, which corresponds to the monohydrate $C_{10}H_7SO_3H{\cdot}H_2O$. The water was taken from a Seral purification system (PURELAB Plus) with a conductivity of about 0.06 μS cm^{-1} and used without any further treatment. APFO (gift from Dyneon 3M, Gendorf) was obtained as aqueous solution with 30% weight content. Either the solution or the solid after evaporation of the water was used. PFOSA, a 50 wt.% aqueous solution, and PFODEA (both from Hoechst AG) were used as received.

Methods

TEM was performed with a Zeiss EM 912 Omega microscope operating at 100 kV. Thin sections were prepared with an Ultracut (Leica) from samples embedded in an acrylic resin (LR White Resin, medium grade, Plano). Scanning electron microscopy (SEM) pictures were obtained with a Gemini 1550 scanning electron microscope (Leo). Light microscopy images were taken with an Olympus BX50 microscope equipped with a CCD camera. Elemental analysis of the fluorine-containing compounds and complexes was carried out in the Fresenius Institute, Berlin, Germany.

Reactions

All reactions were carried out under a ventilation hood in laboratory atmosphere in glass vials with an overall volume of about 15 ml and with an inner diameter of about 2.5 cm. To study its properties, the precipitate formed before starting the polymerization was isolated by filtration, washed with water, and dried under vacuum at room temperature for at least 24 h prior to further investigations.

The general polymerization procedure was as follows: To a solution of NSA in water the fluorosurfactant (either solution or solid) was added, followed by the pyrrole monomer (0.2 ml). During thermal equilibration in an ice bath at 0 °C and before APS addition, a brownish precipitate was formed. After stirring this mixture for some time, 0.2 g of APS dissolved in 1 ml of water was added and the mixture was allowed to react for 1 h. The black polymer was then separated by filtration, washed with water and ethanol, and finally dried under vacuum at room temperature for at least 24 h.

Synthesis of PPY tubes

Into a solution of dopant (0.8 g NSA in 2.4 ml water), 0.2 ml of pyrrole was added, and the mixture was left for 5 min at room temperature under magnetic stirring. Then, the mixture was placed in an ice bath at about 0 °C, still under magnetic stirring, until a precipitate appeared. To start the oxidative polymerization, 0.2 g APS in 1 ml water was slowly added and the mixture was allowed to react for 1 h at about 0 °C under magnetic stirring. The yield after washing relative to the initial mass of pyrrole was about 48%.

Synthesis of PPY squares

APFO (1.5 ml of a 30 wt.% solution) was mixed with a solution of NSA (0.2 g of NSA in 0.5 ml water) and the mixture became immediately thick. After a few seconds under magnetic stirring at room temperature, a white precipitate appeared. After the addition of 0.2 ml of pyrrole under magnetic stirring, the mixture was placed in an ice bath. To start the polymerization after thermal equilibration, 0.2 g of APS dissolved in 1 ml of water was slowly added. The mixture was allowed to react for 1 h before the black polymer was separated by filtration. The yield after washing relative to the initial mass of pyrrole was about 57%.

Synthesis of PPY rings

PFOSA (0.5 g of a 50 wt.% solution) was mixed with a solution of NSA (0.6 g of NSA in 2 ml water). After a few seconds under magnetic stirring at room temperature, a white precipitate appeared. Under magnetic stirring, 0.2 ml of pyrrole was added, and the mixture was placed in an ice bath. The oxidant (0.2 g APS in 1 ml water) was added and the mixture was allowed to react for 1 h at about 0 °C under magnetic stirring. The yield after washing relative to the initial mass of pyrrole was about 53%.

Synthesis of PPY hexagons

Under magnetic stirring, 0.25 g of PFODEA was mixed with a solution of NSA (0.6 g in 2 ml H_2O). Then, 0.2 ml pyrrole was added and the mixture was placed in an ice bath. The oxidant (0.2 g APS in 1 ml water) was added and the mixture was allowed to react for 1 h at about 0 °C under magnetic stirring. The yield after washing relative to the initial mass of pyrrole was about 65%.

Results and discussion

The experimental results are presented mainly in the form of light and electron microscopy images of the corresponding morphologies. Both illustration methods are complementary as light microscopy depicts the wet or dispersed state as obtained from the polymerization and electron microscopy depicts the dry state with more structural details at larger magnification.

This section starts with a short review of the peculiarities of the oxidative pyrrole polymerization and a consideration of the particular reaction conditions of this study which is important for at least a qualitative understanding of the results.

Conditions during the oxidative polymerization of pyrrole

PPY can easily be prepared from aqueous and organic solvents by either chemical or electrochemical oxidative polymerization of pyrrole. This polymerization mechanism has two peculiarities compared with ionic or radical polymerizations. Firstly, the polymer has two identical end groups, that is C_4H_4N-, and secondly, the composition of the repeating unit is different from the monomer, $-C_4H_3N-$ vs C_4H_5N, respectively.

In general, the chemical oxidative polymerization of pyrrole is a redox process where the electron-rich pyrrole (six π-electrons shared by only five atoms) acts as reductant. It seems reasonable to assume that the initial step is the reaction of two pyrrole molecules with one peroxodisulfate ion, as the alternate reaction with a sulfate ion radical $\left(SO_4^{-\bullet}\right)$ requires the thermal dissociation of $S_2O_8^{2-}$, which is, at the reaction temperature of 0 °C, quite unlikely [29]. After the initial dimer formation, the polymerization can proceed either by oxidative dimer coupling or by the addition of pyrrole monomer and subsequently by the coupling of species of any chain length [30].

Besides for chain growth, peroxodisulfate is also consumed for oxidizing the polymer chain, which is called in situ doping, and renders the polymer conducting. The resulting positive charges along the chain are counterbalanced by anions, preferably β-naphthalene sulfate for the recipe considered here. The overall redox equation with APS as oxidant, taking into account the oxidation-polymerization, the oxidative doping process, and the preferential insertion of counterions from the doping agent (here NSA), can be represented as in Scheme 1. Thus, the production of conducting PPY by chemical oxidative polymerization requires an excess of the oxidant depending on the degree of doping. By elemental analysis (carbon-sulfur ratio) it was shown that, under the reaction conditions as applied, 1 NSA unit is attached to about 3.6 pyrrole units [28].

The oxidative polymerizations of pyrrole with APS in aqueous solution with NSA as in situ dopant and fluorosurfactants as additional additives were all carried out with a constant monomer to oxidant molar ratio of 3.3:1. At a glance, this ratio is surprising, as, according to the mechanism of oxidative polymerization (cf. Scheme 1), it does not allow complete pyrrole conversion. But it turned out that this excess of monomer is a prerequisite for the particular outcome of the investigations. At higher concentrations of oxidant, the viscosity of the reaction mixture becomes too high to allow effective stirring with

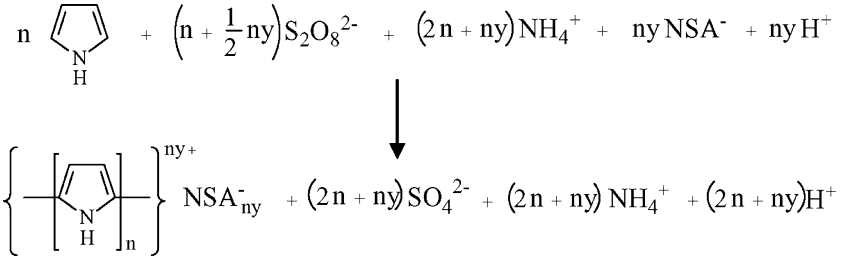

Scheme 1 Overall reaction equation for the PPY synthesis as carried out in this study

Table 1 Characteristic features of the oxidative pyrrole polymerization

Component	Concentration	Implication
NSA	≥0.295 M	pH<<1, acid-base and hydrotropic interaction with pyrrole
APS	≥0.258 M	Strongest contribution to the overall ionic strength and colloidal stability
Fluorosurfactant	≥0.154 M	Concentration >> CMC
Pyrrole	0.847−<1.075 M	No free monomer phase at the beginning, dispersion polymerization
Temperature	0 °C (ice bath)	Necessary for the occurrence of nongranular-shaped PPY

CMC critical micelle concentration

the experimental setup, and the morphology of the polymer is granular. As discussed below, efficient stirring is, besides other conditions, a prerequisite for the observed morphologies.

The water solubility of pyrrole is about 7.5% by weight (1.12 M) [31], which is higher than the highest concentration employed. Moreover, the pyrrole concentration in water can be enhanced due to the hydrotropic action of the NSA [32]. This means that there is no free monomer phase at the beginning, but the polymer, which is insoluble in the continuous phase precipitates, and hence, the polymerization ends as PPY dispersion in water. The reaction as carried out in this study is heterogeneous in nature and possesses characteristic features of the so-called dispersion polymerization technique. The consequences of the individual recipe components on the conditions during the polymerization are listed in Table 1.

From the viewpoint of colloid chemistry, the most important features of these conditions for the polymerization mechanism are the high — in the process, even increasing — ionic strength, which causes a short Debye screening length and facilitates particle encounters, and the high amount of the fluorosurfactants, which is, for all three surfactants, above the critical micelle concentration.

Complex formation in the presence of fluorosurfactants

The reasonable assumption that at least PFOSA might also form a complex with pyrrole, as substitute for NSA as a strong acid is replaced by another strong acid, is not correct. Moreover, the substitution of NSA by any of the perfluoro-compounds does not lead to complex formation with the monomer and consequently, after polymerization, PPY with ordinary granular morphology was obtained. Surprisingly, the formation of platelet-like precipitates was observed between the fluorosurfactants and NSA. For APFO, the platelets exhibit rectangular corners (Fig. 1), whereas for the other surfactants the edges and corners are rounded.

Elemental analysis carried out for the precipitate between NSA and APFO shows that the molar ratios of N to S and F to S are about 6.2:1 and 93.6:1, respectively, indicating that about six APFO molecules interact with one NSA molecule. The driving force and the nature of this interaction are not clear yet. A possible explanation might be that something similar, like a joint salting-out, happens, as the overall ionic strength in this mixture is quite high (1.504 M). The complexes are soluble in common organic solvents like ethanol or dimethylformamide.

The complex formation between NSA and the perfluorosurfactants, that is, the complex formation between two surface active molecules with equally charged hydrophilic head groups (or a neutral and a charged head group in the case of PFODEA), is really surprising. The dimensions of the precipitated objects are up to hundreds of micrometers, which immediately raises questions regarding the arrangements of the molecules. Clearly, these are not mixed micelles where hydrophobic tails jointly forming the core and the head groups point toward the water phase. The complexes must have internal structures, as at least three mutual nonattracting parts of the molecules (the sulfonate groups, the fluorocarbon tail, and the aromatic ring) are confined in the solid. The attractive hydrophobic interaction between the fluorocarbon and the aromatic ring is

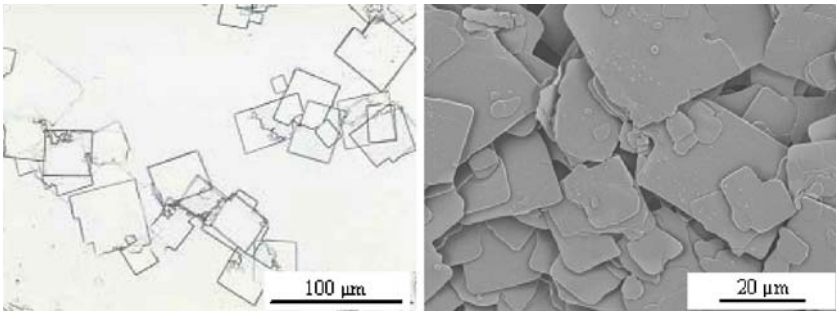

Fig. 1 Light microscopy (*left*) and SEM (*right*) images of APFO-NSA complexes

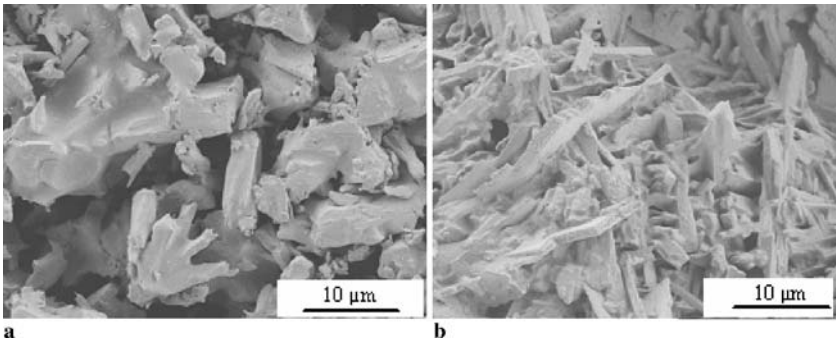

Fig. 2 SEM images of complex particles made of PFOSA, NSA, and pyrrole (**a**) and PFODEA, NSA, and pyrrole (**b**) with initial molar ratios of 0.17:0.9:1 and 0.24:0.9:1, respectively

rather weak, and the formation of internal hydrophilic spots is also likely. Thus, one might expect rather loose arrangement in the complex based on much weaker interactions than for pyrrole-NSA.

The addition of pyrrole monomer alters the complex morphology, except for APFO, from platelet-like to more rod-like morphology, as proven by the SEM images in Fig. 2. These morphologies resemble modified rod-like morphologies as found for the complex between pyrrole and NSA [28]. Elementary analysis data prove that these complexes contain all three partners, that is, the perfluoro-compound, NSA, and the monomer. For example, the nitrogen content of the complex PFOSA-NSA-pyrrole (initial molar ratio 0.17:0.9:1) and the sulfur content of the complex PFODEA-NSA-pyrrole (initial molar ratio 0.24:0.9:1) is 5.20 and 1.5 wt.%, respectively, and in general, the complexes contain between 30 and 40 wt.% of fluorine.

Obviously, the complex between APFO and NSA is more stable than the others, as it is not destroyed upon pyrrole addition. The complex morphology after the addition of pyrrole depends on the ratio of NSA to fluorosurfactants, especially for PFOSA (Figs. 2a and 3) and PFODEA where, with decreasing content of fluorosurfactant, the complex shape becomes more rod-like. This might point to a qualitatively different behavior also during the polymerization reaction.

Oxidative polymerization of pyrrole in the presence of NSA and fluorosurfactants

In general, the light microscopy pictures of Fig. 4 reveal unusual shapes for particles in polymer dispersions, as usually, almost all polymer dispersions after preparation are made of more or less spherical polymer particles. But under the conditions as applied here, dispersions are obtained containing rods, rings, squares, or hexagons. Moreover, there is a strong influence of the nature of the fluorosurfactants on the morphology of the PPY, as instead of rods obtained in the absence of fluorosurfactant, rings, squares, and hexagons are observed for PFOSA, APFO,

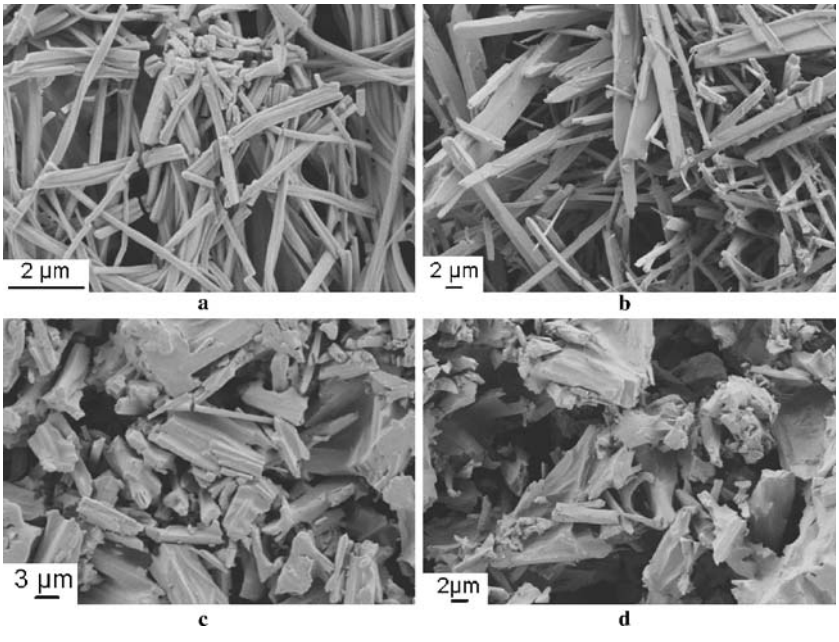

Fig. 3 SEM images of PFOSA-NSA-pyrrole complexes with varying initial amounts of PFOSA and NSA: 0.035:0.9:1 (**a**), 0.07:0.9:1 (**b**), 0.17:2.5:1 (**c**), 0.33:0.9:1 (**d**)

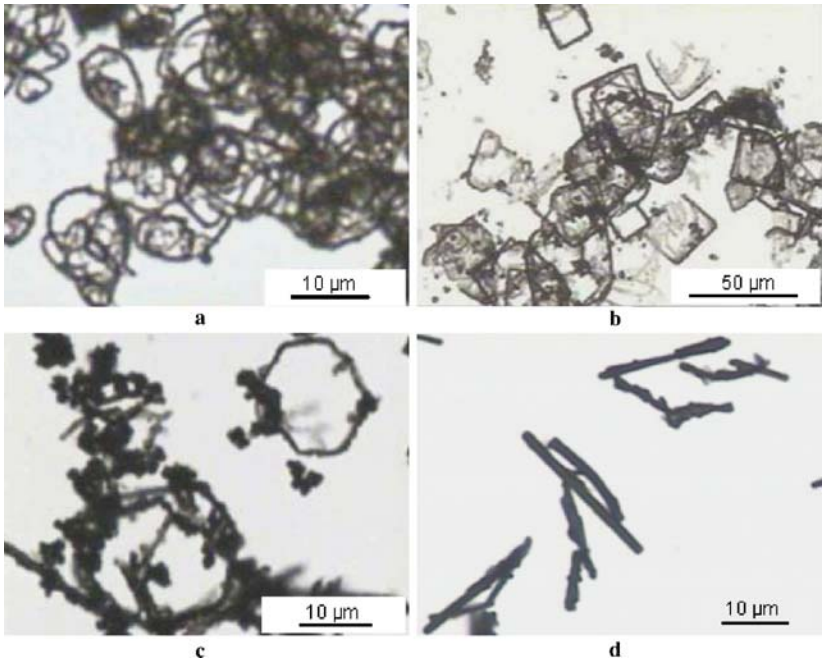

Fig. 4 Light microscopy images of PPY dispersions obtained by oxidative polymerization with APS in the presence of NSA and PFOSA (**a**), NSA and APFO (**b**), NSA and PFODEA (**c**), and with NSA only (**d**); images were taken after washing with ethanol

and PFODEA, respectively. Again, light microscopy provides strong proof that such shaped particles really freely move in the dispersions. SEM images (Fig. 5) reveal more detailed information and show that these structures are aggregates made of almost spherical subunits.

Figure 5d represents a sample taken 30 min after starting the polymerization and washing with water, which is a procedure suited only to removing residual APS and its reaction products, as well as unreacted pyrrole monomer, but not the complex. This image shows illustratively in the lower half what in situ templating means. A smooth complex rod (NSA-pyrrole complex) is only partly covered with PPY-spheres of different sizes. At the end of the polymerization, when the complex rods are completely covered and after washing with ethanol when the precursor complex is dissolved, a PPY tube is left, cf. Diez et al. [28].

Comparing the complex morphologies (Figs. 1, 2 and 3) with those of the polymeric samples (Figs. 4 and 5), the

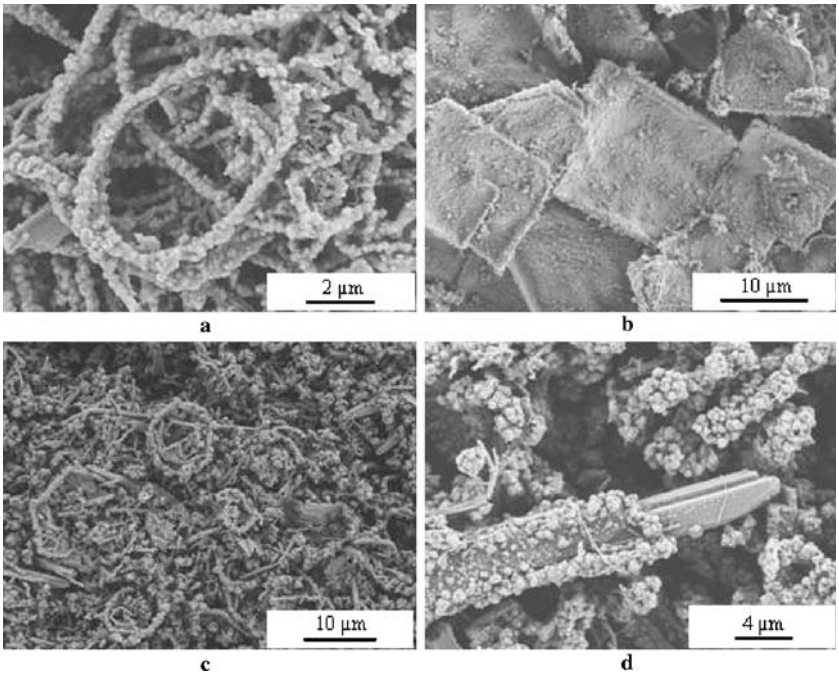

Fig. 5 SEM images of PPY dispersions obtained by oxidative polymerization with APS in the presence of NSA and PFOSA (**a**), NSA and APFO (**b**), NSA and PFODEA (**c**), and with NSA (**d**); images **a**–**c** were taken after washing with ethanol and image **d** after washing with water

Table 2 Morphological variations of PPY plates obtained with changing initial molar ratio of APFO and NSA

APFO (g)	NSA (g)	APFO:NSA	Morphology of PPY
0.60	0	–	Granular
0.45	0.6	1:2.56	Irregular plates
0.45	0.4	1:1.69	Rectangular plates
0.75	0.4	1:1.01	Rectangular frames and plates

conclusion is obvious that the PPY squares are formed in an analogous way like the tubes. However, there is obviously no complex morphology that might serve as template for the rings or hexagons.

Influence of the perfluorosurfactant-NSA concentration ratio

As described for the tubular PPY [28], the specific appearance of the various morphologies depends on the concentration ratio of the reactants, especially the fluorosurfactant and NSA. Tables 2, 3, and 4 and Fig. 6 summarize possible morphological variations of PPY observed when using APFO and PFOSA as fluorosurfactant.

The regularity of the plates depends strongly on the molar ratio of the synergistically acting components APFO and NSA (cf. Table 2). At lower amounts of the perfluoro-compound in this mixture, irregularly formed plates are observed, whereas rectangular plates are formed at higher portions of APFO (cf. Fig. 5b). At approximately equal concentrations, rectangular frames (empty plates) and plates (filled rectangles) are formed (cf. Fig. 6a). If the amount of PFOSA is constant (0.25 g) and the NSA concentration is varied, the morphology of the PPY rings changes, as given in Table 3. For a constant amount of NSA (0.6 g) and a variable amount of PFOSA, the different morphologies of PPY are listed in Table 4.

The disk-morphology as shown in Figs. 6b and 7b was obtained at the highest excess of NSA relative to the amount of PFOSA (Table 4). Under these conditions a few tubes are also formed, as the amount of NSA is so high that the in situ templating mechanism leading to the tubes takes

Table 3 Morphological variations of PPY obtained with changing the initial molar ratio PFOSA and NSA at a given amount of PFOSA (0.25 g)

NSA (g)	PFOSA:NSA (mole)	PPY morphology
0	–	Granular
0.15	1:1.14	Disks
0.45–0.75	1:3.4–1:5.8	Rings
0.9	1:6.8	Broken rings, tubes
1.05	1:8	Broken rings, tubes, belts

Table 4 Morphological variations of PPY obtained with changing the initial molar ratio PFOSA and NSA at a given amount of NSA (0.6 g)

PFOSA (g)	PFOSA:NSA (mole)	PPY morphology
0.05	1:23	Disks, tubes
0.1	1:11.5	Disks
0.18	1:6.4	Disks, rings
0.25	1:4.6	Rings
0.33	1:3.5	Broken rings

place parallel to a mechanism triggered by the PFOSA. Another amazing feature is the concentric alignment of the PPY particles of the secondary hierarchical level inside the filled rectangles (plates) and rings (disks), as shown by the SEM images of Fig. 7. It is remarkable that the particles forming the bended strings are tightly connected to each other, indicating again partial interdiffusion of polymeric chains from touching particles.

Mechanistic contemplations

The strong influence of fluorosurfactants on the PPY morphology during the APS-induced oxidative polymerization in the presence of NSA was observed in this study for the first time. Thus, the focus of the investigations was to explore the field and to unpin interesting points. Nevertheless, some basic conclusions regarding a possible mechanism of formation can be drawn, which will be discussed below.

The essential point is that the nonspherical morphologies, regardless of the particular polymerization recipe, are hierarchically composed. Hence, these tubes, rings, platelets, frames, or squares might be considered as secondary or even tertiary structures clustered together of much smaller PPY structures, as already indicated by the SEM images of Fig. 5. Magnifications as depicted in Fig. 8 reveal secondary structures of almost spherical shape in the size range of about 200–300 nm (Fig. 8a) which are themselves composed of still smaller spherical subunits (primary structures) of only a few nanometers in size (Fig. 8b). The hierarchical morphology of the various PPY particles can be understood considering some colloid-chemical aspects of the oxidative pyrrole polymerization in aqueous media.

The oxidative polymerization of pyrrole as carried out in this study possesses all features of a heterophase polymerization. Despite the absence of a free monomer phase (cf. Table 1) the starting reaction mixture is heterogeneous in nature due to the presence of the particular complex particles. This scenario conditions two important consequences. First, the oxidative polymerization has to start in the continuous phase and second, the polymer chains have to precipitate in the further course of the reaction.

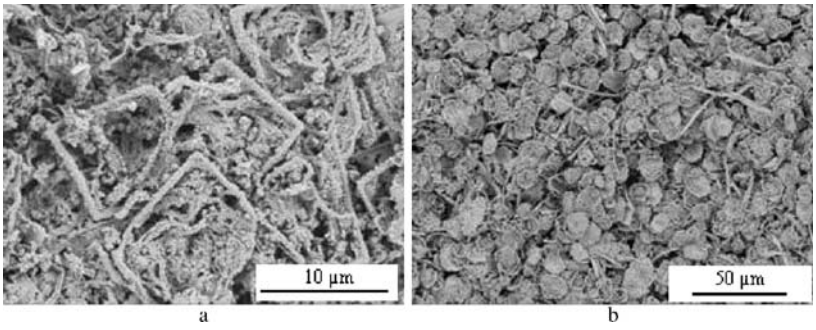

Fig. 6 Illustration of the alignment of PPY particles, initial molar ratio of APFO to NSA of 1:1.01 **(a)** and PFOSA to NSA of 1:23 **(b)**

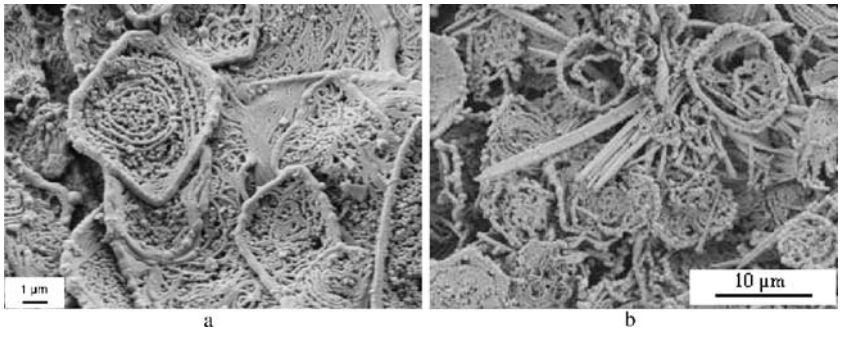

Fig. 7 Illustration of the concentric alignment of PPY particles in squares and rings; initial molar ratio of APFO to NSA of 1:1.69 (**a**) and initial molar ratio of PFOSA to NSA of 1:23 (**b**)

Moreover, the high ionic strength for the various recipes with and without perfluorosurfactants (cf. Table 1) and the resulting Debye-screening length below 0.5 nm favors coagulation of the precipitated PPY particles.

An important aspect of heterophase polymerizations is the degree of swelling of the particles with either monomer or continuous phase. A higher degree of swelling makes the particles softer, and hence, coalescence of particles in coagulation structures is facilitated. To get an idea about the swelling ability of PPY, the uptake of monomer and water by the polymer in the form of powder or as pressed tablet was investigated for samples of different origin. The selection of data as summarized in Table 5 proves that there is a swelling ability of the neat polymer for both liquids (pyrrole and water), whereas the addition of perfluorosurfactant during polymerization reduces the water uptake drastically.

Moreover, these data show that the swelling of the polymer depends on the provenance or the composition, as well as on the consistence of the sample. It is quite reasonable that tablets swell less than powders of the same polymer. It should be mentioned that swelling of pyrrole is quite a fast process, as the mass fraction did not change after 1 h. In any case the equilibrium mass fraction of pyrrole monomer is higher than that of water.

Table 5 Swelling ability of PPY expressed as mass fraction of swelling agent

Provenance/agent	Consistence	Mass fraction (%)
APFO/pyrrole	Powder	38.0
APFO/pyrrole	Tablet	13.8
APFO/water	Tablet	00.0
PFOSA/pyrrole	Powder	58.5
Neat polymer/pyrrole	Tablet	15.0
Neat polymer/water	Tablet	8.0

The provenance of the polymer is indicated by the perfluorosurfactant; neat polymer means PPY polymerized in the absence of any additive; average values of two repeats

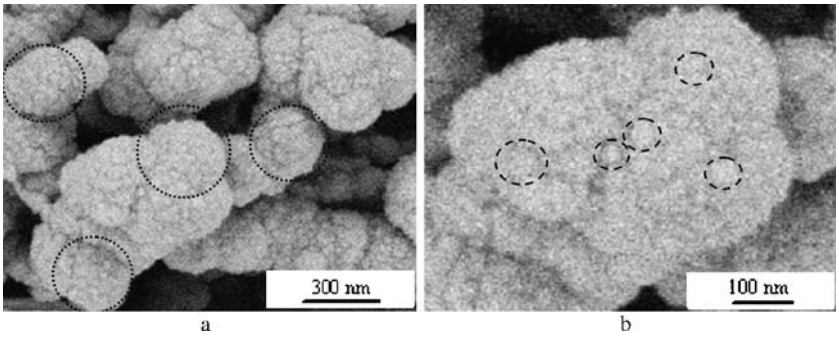

Fig. 8 SEM images of subunits forming the various morphologies depicted in Fig. 5; secondary structures (**a**) and primary structures (**b**) encircled by *dotted* and *dashed lines*, respectively, to guide the eye

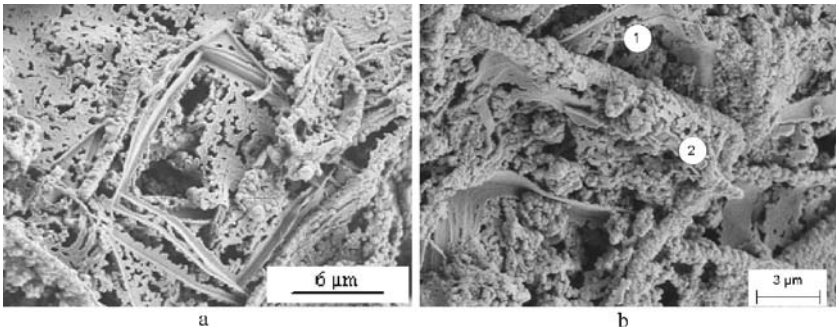

Fig. 9 **a** SEM image showing the smooth side of a partly filled frame prepared with APFO after 15 min polymerization time; **b** SEM image displaying both a smooth (in *region 1*) and a rough (in *region 2*) side of frames; both images were taken after washing with ethanol

The consequences for the development of a certain morphology governed by coagulation and deposition events are noticeable. Contact areas are flattened and the interdiffusion of polymer chains between particles in closest contact is facilitated, thus "gluing" the particles together and stabilizing coagulation structures. The former effect is clearly seen on the SEM images of Fig. 9 (in the middle of Fig. 9a and in region 1 of Fig. 9b), but also on the smooth interior walls of the tubes (cf. Diez et al. [28]).

Additionally, the SEM pictures of Fig. 10 prove quite directly that the formation mechanism of the squares is essentially identical to that described for the PPY tubes (Fig. 5d) by Diez et al. [28]. In either case the initial complex acts as in situ-formed template, and the whole morphology formation process can act this way. The general idea on the mechanism of in situ templating as illustrated by the sketch in Fig. 11 is supported by X-ray diffraction investigations (data not shown here). The X-ray diffraction patterns observed for polymer samples after polymerization, which were washed only with water, correspond to the patterns of the initially formed complex. Contrarily, the polymeric product after washing with ethanol is amorphous.

The in situ templating process is composed of the following steps: Before starting the polymerization, a precipitate (I in Fig. 11) is formed between the NSA, the fluorosurfactant, and the monomer. After the addition of the oxidant (APS) the polymerization reaction starts in the aqueous phase (step a in Fig. 11). At a certain chain length and concentration of PPY chains, particles nucleate from the continuous phase. The deposition of these particles on the surface of the complex is facilitated by the high ionic strength in the continuous phase. At early stages of the polymerization, the density of the PPY particles on the complex surface is still low (II in Fig. 11), and upon dissolving the template by washing with water and, subsequently, ethanol (step b in Fig. 11), either individual polymer particles or aggregates can be observed. Note that the particles do not exhibit spherical symmetry, as the side of the particles that was attached to the template is flattened. At longer polymerization times (III in Fig. 11), the PPY particles cover the template completely. Now, if the template is dissolved by washing with ethanol, the

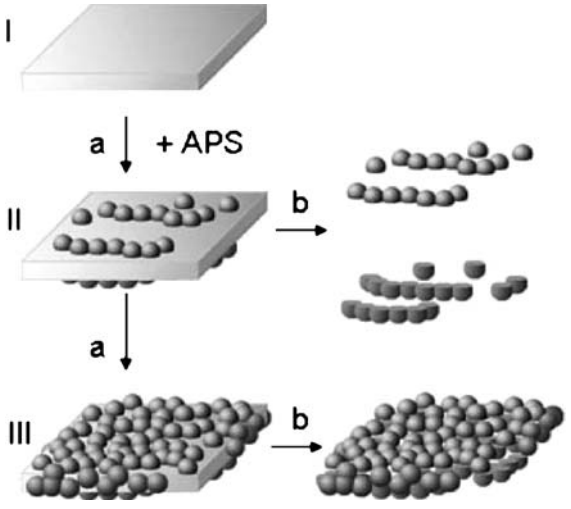

Fig. 11 Schematic illustration of the in situ templating oxidative polymerization of pyrrole in the presence of NSA and APFO

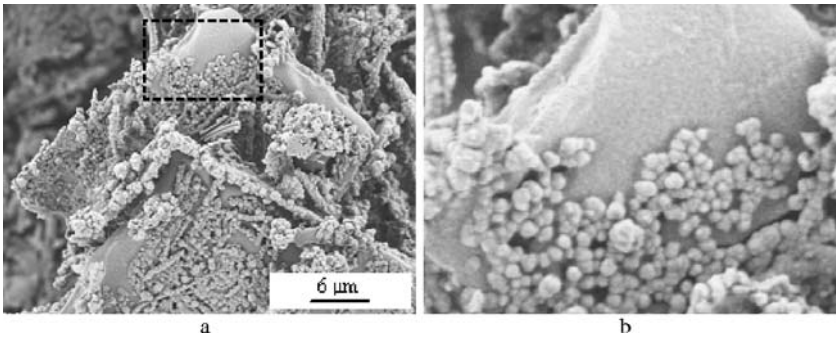

Fig. 10 SEM images illustrating the formation of PPY squares; samples were taken after a polymerization time of 30 min and washed with water only; **b** magnification of the encircled area of picture **a**

particle shell around the template cannot be destroyed as the particles glue together due to the partial interdiffusion of polymer chains from swollen neighboring particles.

Among the various morphologies, the PPY rings obtained in the presence of PFOSA are obviously a special case, as the shape of the corresponding complex does not fit, i.e., it is not ring-like. A detailed analysis of the morphology changes that occur during the polymerization (cf. Fig. 12) could resolve this apparent contradiction to the idea of in situ templating.

The morphology of the complex formed between NSA and PFOSA during the preparation of the reaction mixture (stage I in Fig. 12) changes after the addition of pyrrole monomer, as shown by the sequence of images "a–c." Along with the change of the morphology, the composition of the complex also changes as the particles of image b already contain pyrrole (cf. above elemental analysis data). Obviously, the acid-base interaction between NSA and pyrrole is much stronger than the interaction in the initially formed precipitate. Eventually, the morphology of the NSA-PFOSA complex alters from plates to threads, which can be up to hundreds of micrometers long and less than 50 nm thick. Similar changes also occur during the first minutes after APS addition (stage II in Fig. 12), as illustrated by the sequence of images "a" and "d–f." In this stage of the polymerization, the thickness of the threads decreases and their number increases rapidly. Although an experimentally proven reason for the decomposition of the belts (image "d") into fibers (images "e" and "f") cannot be given at the moment, the assumption seems to be fair that the driving force arises from the oleophobic nature of the perfluoroalkyl chains, which try to minimize the contact area not only with water but also with pyrrole. The sulfonate groups are, even under the strongly acidic

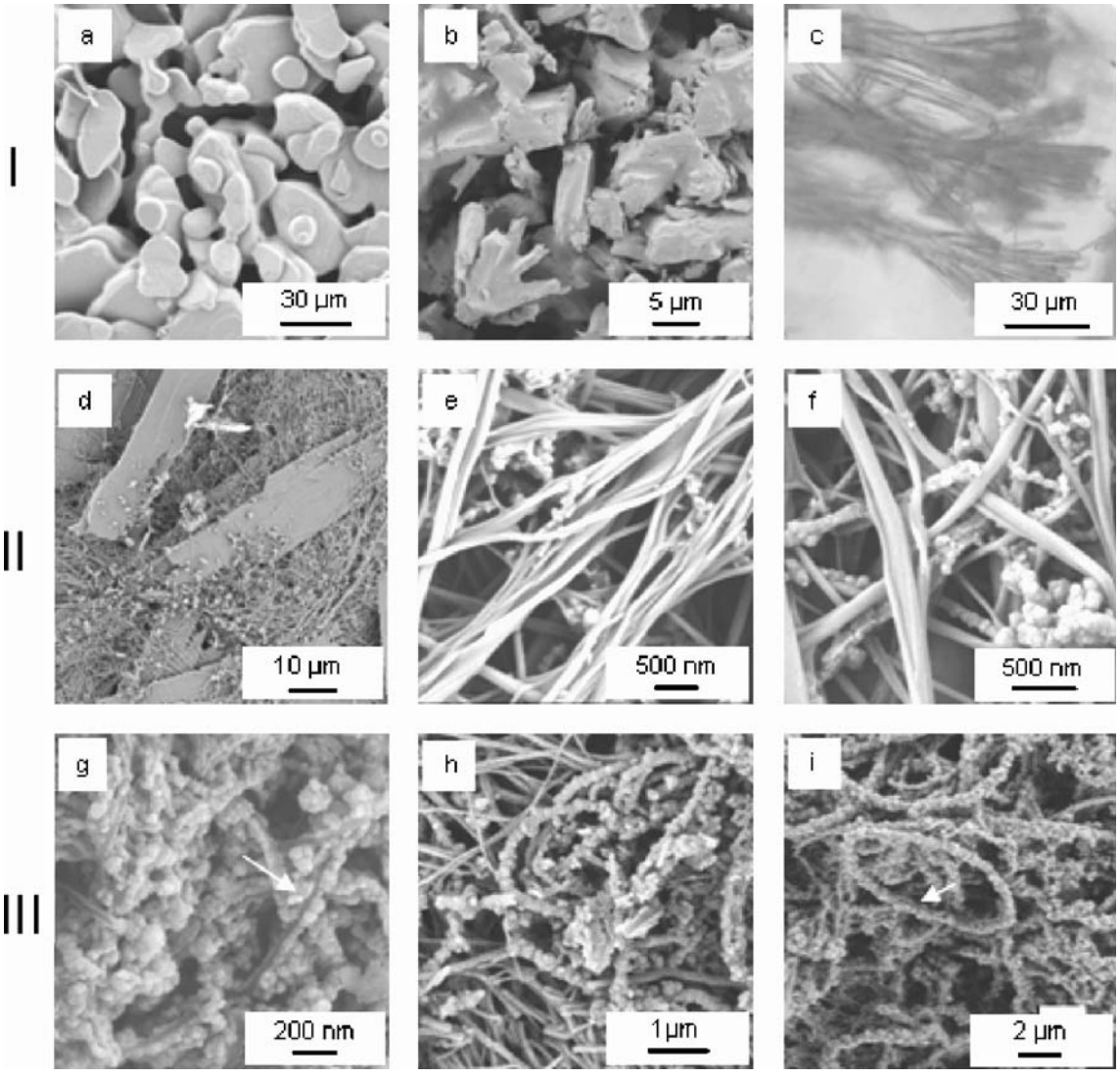

Fig. 12 Sequence of images illustrating morphological changes during pyrrole polymerization in the presence of PFOSA

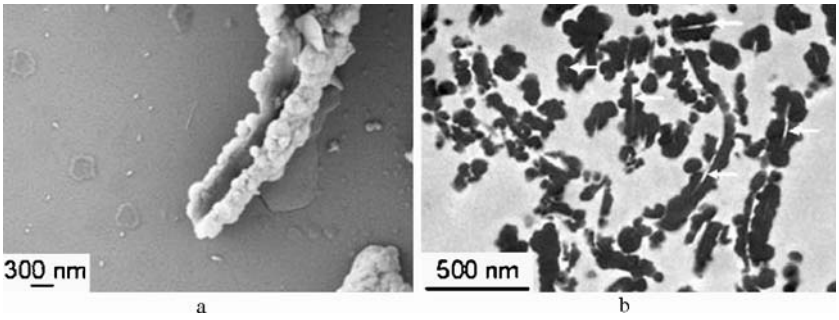

Fig. 13 SEM image (**a**) and TEM image (**b**) of microtomed cross section showing the groove inside the ring-forming PPY coagulation structure; sample for image **a** synthesized in the presence of 0.33 g PFOSA and 0.6 g NSA, sample for image **b** obtained with 0.25 g PFOSA and 0.6 g NSA

conditions, able to stabilize the larger interface. Moreover, these pictures show that particles deposit on the thin and, apparently, very flexible fibers. It is reasonable to assume that the deposited particles cause the fibers to bend and eventually cause the ring-closure later during the polymerization (stage III in Fig. 12). In the regions of images "g" and "i" of Fig. 12 indicated by the arrows, a groove along the inner perimeter of the rings is visible, which supports the idea of bending threads as templates. The SEM image of Fig. 13a shows such a groove in a piece of a broken PPY ring as obtained after treating the cleaned dispersion with ultrasound. Note that an ultrasound of medium power breaks the rings but does not lead to deagglomeration into secondary or primary PPY spheres, which are, obviously, quite strongly glued together. The grooves were also visible in thin sections of microtomed samples. In Fig. 13b, the particular regions in cut parts of rings are indicated by arrows.

Concerning the reason for the concentric alignment of the PPY particles inside the squares and rings (cf. Fig. 7), only speculations are possible with the presently available experimental data. Nevertheless, it is likely that the particular alignment is at least supported by the hydrodynamic fields in the reaction mixture. It is known that polystyrene latex particles form in shear field string-like coagulation structures (so-called orthokinetic coagulation), whereas under the conditions of perikinetic coagulation (in the absence of an external shear field where the particles move only by Brownian motion), spherical arrangements result [33].

Moreover, as the particles are made of conducting PPY (they contain the ionic compounds NSA and PFOSA as dopants), a dipole moment can easily be induced, which in turn also favors the chain-like aggregates in the presence of a directed motion, as proven for dust particles [34, 35]. Accordingly, the secondary PPY particles align in the continuous phase under the influence of electrical charges and the shear field before deposit on the template surface. Note that the polarization of the particles might support the ring closure as well.

In summary, the mechanism of the formation of PPY particles with special morphologies, such as tubes, rings, disks, squares, and rectangular frames, during the oxidative pyrrole polymerization with APS can be described as the result of specific colloid-chemical interactions triggered by the particular polymerization conditions (high ionic strength, the presence of fluorosurfactants and NSA) and the presence of templates, which are formed prior to polymerization due to the specific interaction of recipe components.

Acknowledgements The authors are indebted to Rona Pitschke and Heike Runge for taking the electron microscopy images and to Sylvia Pirok for standard elemental analysis. I. Díez thanks the Max Planck Institute of Colloids and Interfaces for hosting and the allowance to use the necessary equipment and analytical techniques.

References

1. Diaz AF, Castillo JI, Logan JA, Lee WY (1981) J Electroanal Chem Interfacial Electrochem 129:115
2. Gerritsen M, Jansen JA, Kros A, Nolte RJ, Lutterman JA (1998) J Invest Surg 11:163
3. Skotheim TA, Elsenbaumer RL, Reynolds JR (1998) Handbook of conducting polymers, 2nd edn, revised and expanded. Dekker, New York
4. Yin W, Li J, Li Y, Wu J, Gu T (2001) J Appl Polym Sci 80:1368
5. Wessling B (2005) Synth Met 152:5
6. Shen Y, Wan M (1998) Synth Met 96:127
7. Sahin Y, Aydin A, Udum YA, Pekmez K, Yildiz A (2004) J Appl Polym Sci 93:526
8. Jang J, Oh JH (2003) Polym Mater Sci Eng 89:397
9. Jang J, Oh JH, Stucky GD (2002) Angew Chem Int Ed Engl 41:4016
10. John R, John MJ, Wallace GG, Zhao H (1992) Symposium on Electrochemistry in Microheterogeneous Fluids, p 225
11. Zhang X, Zhou L, Wen M, Liang H, Zhang J, Liu Z (2005) J Phys Chem B 109:1101
12. Arca E, Cao T, Webber SE, Munk P (1994) Polym Prepr 35:334
13. Goren M, Lennox RB (2001) Nano Lett 1:735
14. Kudoh Y, Akami K, Matsuya Y (1998) Synth Met 98:65
15. Yoo SI, Sohn B-H, Zin W-C, Jung JC (2004) Langmuir 20:10734

16. Carswell ADW, Genetti WB, Wei X, Grady BP (1999) 218th ACS national meeting, COLL 239, New Orleans, 22–26 August 1999
17. Ishizu K, Tanaka H, Saito R, Maruyama T, Yamamoto T (1996) Polymer 37:863
18. Akami K, Kudo Y, Kusayanagi H, Matsuya Y (2001) Japanese patent 2001283655
19. Shapiro JS, Smith WT (1993) Polymer 34:4336
20. Shapiro JS, Smith WT, MacRae C (1995) Polymer 36:1133
21. Subianto S, Will GD, Kokot S (2005) Int J Polym Mater 54:141
22. Lee S, Sung H, Han S, Paik W (1994) J Phys Chem 98:1250
23. Fou AC, Rubner MF (1995) Macromolecules 28:7115
24. Huang ZY, Wang PC, MacDiarmid AG, Xia YN, Whitesides G (1997) Langmuir 13:6480
25. Marinakos SM, Novak JP, Brousseau LC 3rd, House AB, Edeki EM, Feldhaus JC, Feldheim DL (1999) J Am Chem Soc 121:8518
26. Bartlett PN, Birkin PR, Ghanem MA, Toh C-S (2001) J Mater Chem 11:849
27. Cassagneau T, Caruso F (2002) Adv Mater 14:1837
28. Diez I, Tauer K, Schulz B (2004) Colloid Polym Sci 283:125
29. Behrmann EJ, Edwards JO (1980) Rev Inorg Chem 2:179
30. Street GB, Clarke TC, Geiss RH, Lee VY, Nazzal A, Pfluger P, Scott JC (1983) J Phys (Paris) C3(44):599
31. Jasne S (1988) In: Kroschwitz JI (ed) Encyclopedia polymer science and engineering, vol 13. Wiley, New York, p 42
32. Hons G (1996) In: Stache HW (ed) Anionic surfactants, vol 56. Marcel Dekker, New York, p 39
33. Ali SI, Zollars RL (1987) J Colloid Interface Sci 117:425
34. Lapenta G (1998) Phys Scr 57:476
35. Praburam G, Goree J (1995) Astrophys J 441:830